



# Polarized Raman study on phase transitions in $0.24\text{Pb}(\text{In}_{1/2}\text{Nb}_{1/2})\text{O}_3-0.43\text{Pb}(\text{Mg}_{1/3}\text{Nb}_{2/3})\text{O}_3-0.33\text{PbTiO}_3$ single crystal

Fengmin Wu<sup>a,b</sup>, Bin Yang<sup>a</sup>, Enwei Sun<sup>a</sup>, Rui Zhang<sup>a</sup>, Dapeng Xu<sup>c</sup>, Jing Zhou<sup>c</sup>, Wenwu Cao<sup>a,d,\*</sup>

<sup>a</sup> Condensed Matter Science and Technology Institute, Harbin Institute of Technology, Harbin 150080, China

<sup>b</sup> College of Applied Science, Harbin University of Science and Technology, Harbin 150080, China

<sup>c</sup> School of Physics, Jilin University, Changchun 130023, China

<sup>d</sup> Materials Research Institute, The Pennsylvania State University, University Park, PA 16802, USA

## ARTICLE INFO

### Article history:

Received 7 June 2012

Received in revised form 9 October 2012

Accepted 9 October 2012

Available online 17 October 2012

### Keywords:

PIN–PMN–PT

Micro-Raman

Phase transitions

## ABSTRACT

Polarized Raman spectroscopy was performed to investigate the local lattice structure and phase transitions of unpoled  $0.24\text{Pb}(\text{In}_{1/2}\text{Nb}_{1/2})\text{O}_3-0.43\text{Pb}(\text{Mg}_{1/3}\text{Nb}_{2/3})\text{O}_3-0.33\text{PbTiO}_3$  ( $0.24\text{PIN}-0.43\text{PMN}-0.33\text{PT}$ ) single crystal in the temperature range from 30 °C to 260 °C.  $M_A$ - and  $M_C$ -type monoclinic phases were detected by micro-Raman spectra measured in different micro areas. Temperature dependence of Raman intensities, frequency shifts, mode merge and intensity ratios in the  $VV$  and  $VH$  geometries were investigated. Our results indicated that the monoclinic–tetragonal ( $M-T$ ) phase transition of the ternary relaxor-based ferroelectric single crystal  $0.24\text{PIN}-0.43\text{PMN}-0.33\text{PT}$  occurs at 85 °C, which is verified by the mode merging from 520  $\text{cm}^{-1}$  and 580  $\text{cm}^{-1}$  to 500  $\text{cm}^{-1}$ , and the tetragonal–cubic ( $T-C$ ) phase transition happens at 200 °C based on the vanishing mode at 780  $\text{cm}^{-1}$  measured in the  $VH$  polarization.

© 2012 Elsevier B.V. All rights reserved.

## 1. Introduction

Relaxor-based ternary ferroelectric single crystals  $(1-x-y)\text{Pb}(\text{In}_{1/2}\text{Nb}_{1/2})\text{O}_3-y\text{Pb}(\text{Mg}_{1/3}\text{Nb}_{2/3})\text{O}_3-x\text{PbTiO}_3$  (PIN–PMN–PT) have attracted much attention in recent years for their excellent piezoelectric properties and their potential applications in ultrasonic transducers and actuators [1–6]. It was reported that PIN–PMN–PT single crystals have about 30 °C higher Curie temperature and 2.5 times higher coercive field compared with their binary counterpart  $(1-x)\text{Pb}(\text{Mg}_{1/3}\text{Nb}_{2/3})\text{O}_3-x\text{PbTiO}_3$  (PMN–PT) with just as excellent piezoelectric and optical properties [3,4,6]. These outstanding properties are enhanced near the morphotropic phase boundary (MPB), which is located at  $x = 0.33$ , for both PMN–PT and PIN–PMN–PT solid solution single crystals. The giant electromechanical response of relaxor-based ferroelectric single crystals has been attributed to polarization rotation in the lower symmetry intermediate monoclinic phase in the MPB region at room temperature [7–9]. The widely used characterization methods such as dielectric spectroscopy and polarized optical microscopy, can only reveal the macroscopic properties of crystals. In order to verify the microscopic symmetry, one needs to perform microscopic level measurements.

Raman spectroscopy is a convenient microprobe to study the local lattice structure and phase transitions in ferroelectric materials [11–17]. Up to date, Raman study on the ternary relaxor-based

ferroelectric PIN–PMN–PT single crystals has not been reported. In this work, the temperature dependence of polarized micro-Raman spectra of unpoled  $[001]_c$ -oriented  $0.24\text{PIN}-0.43\text{PMN}-0.33\text{PT}$  single crystal has been investigated to analyze the crystal structures and phase transitions.

## 2. Experiments

High-quality PIN–PMN–PT single crystal used in this work was grown by the modified Bridgman method [3]. The composition along the growth direction varies due to the segregation of titanium in the crystal. The single crystal used for Raman measurements is  $0.24\text{PIN}-0.43\text{PMN}-0.33\text{PT}$  with the MPB composition. The sample was oriented by the Laue back reflection machine [10] with an accuracy of  $\pm 0.5^\circ$  and cut along the main crystallographic directions  $[100]_c \times [010]_c \times [001]_c$  based on the pseudo-cubic coordinates. The dimensions of the sample are  $7.0^x \times 3.0^y \times 0.6^z$  mm<sup>3</sup> and the two (001) faces were polished to optical quality. The polarized Raman spectra in the wave numbers ranging from 150  $\text{cm}^{-1}$  to 1000  $\text{cm}^{-1}$  were taken by a Jobin Yvon HR800 micro-Raman spectrometer using the 514.5 nm excitation line from an argon ion laser (Spectra Physics Stablite 2017). The incident and scattered lights propagated along  $[001]_c$  ( $z$ -direction), and the polarization direction of the incident light was parallel to the  $[010]_c$  ( $y$ -direction). The spectra were recorded both in the parallel ( $VV$ )  $z(yy)\bar{z}$  and the crossed ( $VH$ )  $z(yx)\bar{z}$  polarization geometries, where  $x$ ,  $y$ , and  $z$  are the pseudo-cubic axes. The Raman resolution is 0.5  $\text{cm}^{-1}$  and the laser with power of 2 mW was focused on the sample surface with a  $50\times$  long focus objective lens. The temperature on the sample was controlled from 30 °C to 260 °C using a Linkam TS600 hot stage with a temperature stability of  $\pm 0.1$  °C.

## 3. Results and discussion

It was reported that the relaxor-based ferroelectric single crystals with MPB composition are in the monoclinic phase at room

\* Corresponding author at: Materials Research Institute, The Pennsylvania State University, University Park, PA 16802, USA

E-mail addresses: binyang@hit.edu.cn (B. Yang), dzk@psu.edu (W. Cao).

temperature. Based on the polarized microscopy observation, the coexistence of  $M_A$  and  $M_C$  phases had been observed in 0.68PMN–0.32PT single crystal [8]. The structures of 0.68PMN–0.32PT and 0.92PZN–0.08PT single crystal was confirmed as in monoclinic phase using X-ray diffraction and micro-Raman spectroscopy [17,18].

Fig. 1 depicts the polarized micro-Raman spectra measured in different micro areas (a)–(c) on the (001) face of 0.24PIN–0.43PMN–0.33PT single crystal. The modes around  $270\text{ cm}^{-1}$ ,  $430\text{ cm}^{-1}$ ,  $500\text{ cm}^{-1}$ ,  $570\text{ cm}^{-1}$  and  $780\text{ cm}^{-1}$  can be seen clearly in the spectra. As shown in Fig. 1, the Raman peaks in the range  $500\text{--}800\text{ cm}^{-1}$  exhibit obvious region dependence. There are little different in  $VV$  and  $VH$  Raman spectra in area (a), which is the typical feature of the  $M_A$ -type monoclinic structure. However, in area (c), the peak at  $570\text{ cm}^{-1}$  in the  $VH$  geometry is only a weak shoulder, while the broad band centered at  $780\text{ cm}^{-1}$  is very weak relative to that in the  $VV$  geometry. Such features suggest that the structure of this micro-area is in the  $M_C$ -type monoclinic phase [14]. In the present work, we select (a) area to discuss the phase transition of 0.24PIN–0.43PMN–0.33PT single crystal.

The polarized micro-Raman spectra at the temperature from  $30\text{ }^\circ\text{C}$  to  $210\text{ }^\circ\text{C}$  are shown in Fig. 2. There exists obvious intensity changing, mode merging and frequency shift with the increase of temperature. Each Raman mode has a certain Raman tensor, which determines the appearance of Raman modes in a given polarization configuration according to the Raman selection rules. The intensities and mode shapes of Raman spectra strongly depend on the polarization configurations and the crystal orientation. It means that the variations of the lattice structure and the crystalline orientations of the micro-domain in the sample determine the regional diversity of the micro-Raman spectra. When the temperature is lower than  $85\text{ }^\circ\text{C}$ , clear changes take place in the  $VH$  geometry. The mode intensity of  $780\text{ cm}^{-1}$  is decreasing upon heating, and red shift occurs for the modes at  $520\text{ cm}^{-1}$  and  $580\text{ cm}^{-1}$ . At  $85\text{ }^\circ\text{C}$ , the mode at  $580\text{ cm}^{-1}$  starts to merge into the mode at  $520\text{ cm}^{-1}$  as shown in Fig. 2(b), and both modes merge to  $500\text{ cm}^{-1}$  when the temperature reaches  $121\text{ }^\circ\text{C}$ . At the same time, the mode intensity of  $780\text{ cm}^{-1}$  shows a clear decrease. According to the group theory analysis, there are 12 Raman-active vibration modes in the monoclinic structure classified as  $8A'$  and  $4A''$  [19]. The Raman modes located at  $580\text{ cm}^{-1}$  and  $780\text{ cm}^{-1}$  are assigned to  $A'$  modes, while the modes around  $270\text{ cm}^{-1}$  and  $520\text{ cm}^{-1}$  are attributed to  $A''$  modes. In point group classification, monoclinic phase  $C_s$  is a subgroup of both  $C_{4v}$  of the tetragonal phase and  $C_{3v}$  of rhombohedral phase. When the monoclinic–tetragonal (M–T)

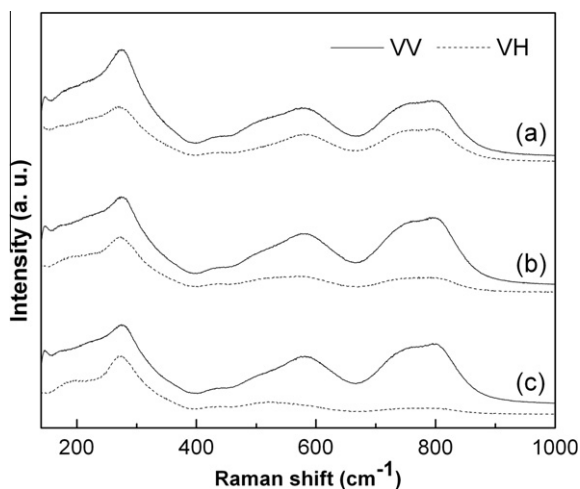


Fig. 1. Polarized micro-Raman spectra measured from different micro-areas on the (001) surface of a 0.24PIN–0.43PMN–0.33PT single crystal.

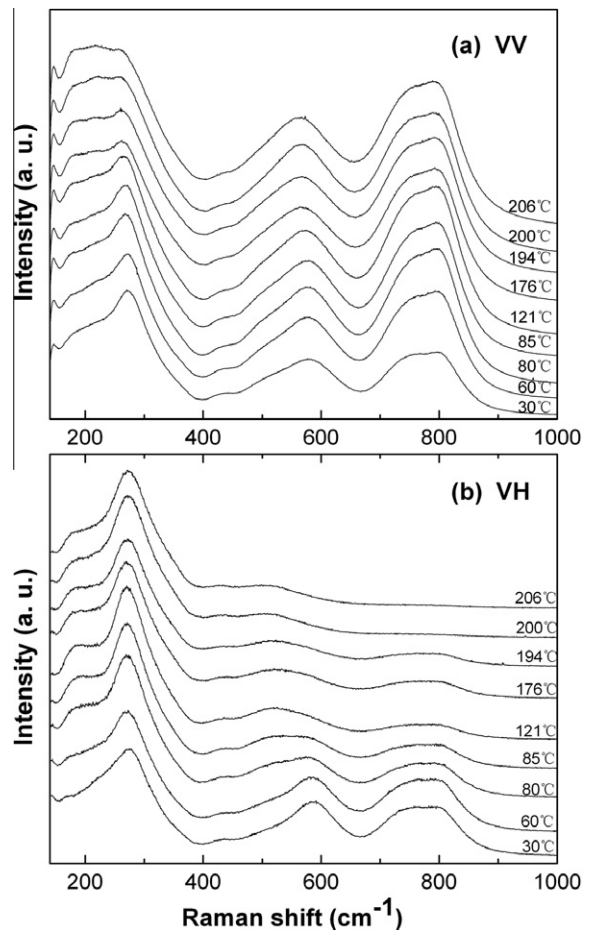
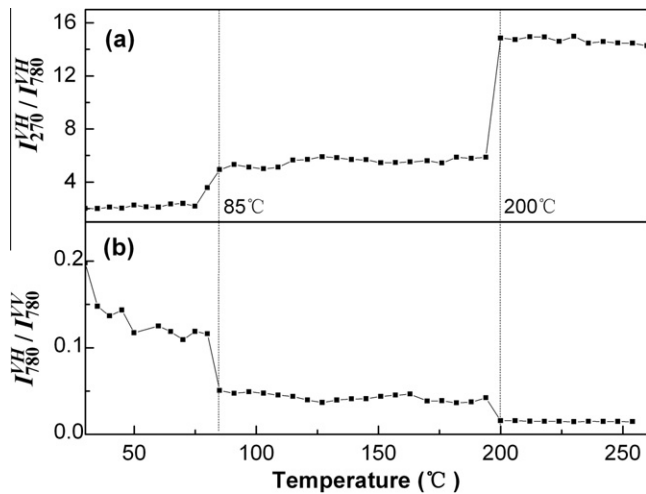


Fig. 2. Polarized micro-Raman spectra of 0.24PIN–0.43PMN–0.33PT single crystal at the temperature from  $30\text{ }^\circ\text{C}$  to  $210\text{ }^\circ\text{C}$  in (a)  $VV$  and (b)  $VH$  geometries.

phase transition takes place,  $A'$  and  $A''$ , belonging to the monoclinic structure, will transform into  $B_1$  and  $E$  modes of the tetragonal phase, respectively [19]. At  $121\text{ }^\circ\text{C}$ , the mode at  $500\text{ cm}^{-1}$  in the  $VH$  geometry is associated with the  $E(3T_0)$  phonon mode in the tetragonal phase according to the Raman selection rules. Thus, the mode transformation from  $520\text{ cm}^{-1}$  and  $580\text{ cm}^{-1}$  to  $500\text{ cm}^{-1}$  implies a phase transition from the monoclinic to tetragonal phase.

When the temperature increases from  $85\text{ }^\circ\text{C}$  to  $210\text{ }^\circ\text{C}$  in the  $VV$  geometry, the mode at  $270\text{ cm}^{-1}$  has an obvious redshift as shown in Fig. 2(a). The redshift of the mode at  $270\text{ cm}^{-1}$ , assigned as the O–B–O bending mode in 0.24PIN–0.43PMN–0.33PT single crystal, is similar to other perovskite relaxor-based ferroelectrics single crystals, which suggests the enhancement of local ordering [20]. In the  $VH$  geometry, both the  $500\text{ cm}^{-1}$  and  $780\text{ cm}^{-1}$  modes become weaker as shown in Fig. 2(b). Especially, the  $780\text{ cm}^{-1}$  mode exhibits strong temperature and polarization dependence. It becomes weaker in the  $VH$  geometry with increasing temperature and vanished at about  $200\text{ }^\circ\text{C}$ . However, the temperature change of this mode in  $VV$  geometry is not so obvious. Therefore, this mode may be assigned as  $A_{1g}$  since it only exists in the  $VV$  geometry at high temperature [17]. The disappearing of the  $780\text{ cm}^{-1}$  mode in the  $VH$  geometry reveals a phase transition from the tetragonal (T) to cubic (C) phase. Therefore, the T–C phase transition of 0.24PIN–0.43PMN–0.33PT happens at  $200\text{ }^\circ\text{C}$  [21,22].

It has been realized that the ratio of band intensities depends on the domain wall structure in the region where the laser beam is focused [23]. The ratio of the intensities between the mode of



**Fig. 3.** The temperature evolution of the Raman modes intensity ratio. (a) The ratio of the intensity between the mode at  $270\text{ cm}^{-1}$  and  $780\text{ cm}^{-1}$  in  $VH$  geometry. (b) The intensity ratio of the crossed to the parallel component of the mode at  $780\text{ cm}^{-1}$ .

$270\text{ cm}^{-1}$  and  $780\text{ cm}^{-1}$  in  $VH$  geometry as a function of temperature is shown in Fig. 3(a). It can be seen that the ratio  $I_{270}^{VH}/I_{780}^{VH}$  increases sharply at  $80^\circ\text{C}$  and reaches a stable value at  $85^\circ\text{C}$ , which is the M–T phase transition temperature. The ratio remains at a stable value with further increase of temperature and a sudden increase happens at  $200^\circ\text{C}$ , which indicates the T–C phase transition. The mode at  $780\text{ cm}^{-1}$  corresponds to the Nb–O–Mg and Nb–O–In stretching mode, which is similar to the Nb–O–Mg stretching mode in PMN–PT and Nb–O–Zn stretching mode in PZN–PT single crystals [13]. It was reported that the decrease in the intensity of this stretching mode indicates the reduction of ordered domains [20].

Fig. 3(b) presents the temperature dependence of the intensity ratio of the crossed component  $VH$  to the parallel component  $VV$  of the  $780\text{ cm}^{-1}$  band  $I_{780}^{VH}/I_{780}^{VV}$ , which more clearly depict the behavior of the mode at  $780\text{ cm}^{-1}$ . It was confirmed that the temperature evolution of this intensity ratio  $I_{780}^{VH}/I_{780}^{VV}$  can indicate phase transitions in the relaxor-based ferroelectric materials [22,24]. Fig. 3(b) shows that upon heating, the intensity ratio decreases as a whole in the M phase, remains stable in the T phase and reaches the lowest value in the C phase.

#### 4. Conclusion

Polarized micro-Raman spectra of the unpoled 0.24PIN–0.43PMN–0.33PT single crystal have been systematically measured in the temperature range from  $30^\circ\text{C}$  to  $260^\circ\text{C}$ .  $M_A$ - and  $M_C$ -type

monoclinic phases were detected by micro-Raman spectra measured in different micro areas. With increasing temperature, two phase transitions happened at  $85^\circ\text{C}$  and  $200^\circ\text{C}$  from monoclinic to tetragonal and from tetragonal to cubic, respectively. The temperature dependence of the intensity ratios, frequency shifts of some Raman modes also provide clear evidence for the sequences of the phase transitions in 0.24PIN–0.43PMN–0.33PT.

#### Acknowledgments

This research was supported by the National key Basic Research Program of China (973 Program) under Grant No. 2013CB632900, the NIH under Grant No. P41-EB21820, the National Nature Science Foundation of China under Grant No. 10704021. High quality 0.24PIN–0.43PMN–0.33PT single crystal was provided by the H.C. Materials Inc., Bolingbrook, IL, USA.

#### References

- [1] Y. Hosono, Y. Yamashita, H. Sakamoto, N. Ichinose, *Jpn. J. Appl. Phys., Part 1* 42 (2003) 5681–5686.
- [2] D. Lin, Z. Li, F. Li, Z. Xu, X. Yao, *J. Alloys Comp.* 489 (2010) 115–118.
- [3] S. Zhang, J. Luo, W. Hackenberger, T.R. Shrout, *J. Appl. Phys.* 104 (2008) 064106–064110.
- [4] E. Sun, S. Zhang, J. Luo, T.R. Shrout, W. Cao, *Appl. Phys. Lett.* 97 (2010) 032902–032904.
- [5] H. Chen, Z. Liang, L. Luo, Y. Ke, Q. Shen, Z. Xia, C. Jiang, J. Pan, *J. Alloys Comp.* 518 (2012) 63–67.
- [6] S. Zhang, J. Luo, W. Hackenberger, N.P. Sherlock, R.J. Meyer Jr., T.R. Shrout, *J. Appl. Phys.* 105 (2009) 104506–104510.
- [7] B. Noheda, D.E. Cox, G. Shirane, R. Guo, B. Jones, L.E. Cross, *Phys. Rev. B* 63 (2000) 014103–014111.
- [8] Z. Wang, Rui Zhang, E. Sun, W. Cao, *J. Alloys Comp.* 527 (2012) 101–105.
- [9] J. Li, G. Rao, G. Liu, J. Chen, L. Lu, X. Jing, S. Li, J. Liang, *J. Alloys Comp.* 425 (2006) 373–378.
- [10] R. Shukla, K.K. Rajan, P. Gandhi, L.C. Lim, *Appl. Phys. Lett.* 92 (2008) 212907–212909.
- [11] M. El Marssi, R. Farhi, Y.I. Yuzyuk, *J. Phys.: Condens. Matter* 10 (1998) 9161–9171.
- [12] H. Bouyanfif, M. El Marssi, N. Lemeé, F. Lemarrec, M.G. Karkut, B. Dkhil, Y.I. Yuzyuk, *Eur. Phys. J. B* 85 (2012) 35.
- [13] M. Shen, G.G. Siu, Z.K. Xu, W. Cao, *Appl. Phys. Lett.* 86 (2005) 252903–252905.
- [14] Y. Yang, Y.L. Liu, S.Y. Ma, K. Zhu, L.Y. Zhang, J. Cheng, G.G. Siu, Z.K. Xu, H.S. Luo, *Appl. Phys. Lett.* 95 (2009) (1913) 051911–051913.
- [15] M. El Marssi, H. Dammak, *Solid State Commun.* 142 (2007) 487–491.
- [16] Y. Yang, Y.L. Liu, L.Y. Zhang, K. Zhu, S.Y. Ma, G.G. Siu, Z.K. Xu, H.S. Luo, *J. Raman Spectrosc.* 41 (2010) 1735–1742.
- [17] J. Cheng, Y. Yang, Y.H. Tong, S.B. Lu, J.Y. Sun, K. Zhu, Y.L. Liu, G.G. Siu, Z.K. Xu, *J. Appl. Phys.* 105 (2009) 053519–053523.
- [18] B. Noheda, D.E. Cox, G. Shirane, *Phys. Rev. B* 66 (2002) 054104–054113.
- [19] K.C.V. Lima, A.G.S. Filho, A.P. Ayala, J.M. Filho, P.T.C. Freire, F.E.A. Melo, E.B. Araujo, J.A. Eiras, *Phys. Rev. B* 63 (2001) 184105–184109.
- [20] E. Husson, L. Abello, A. Morell, *Mater. Res. Bull.* 25 (1990) 539–545.
- [21] J.Y. Sun, Y.L. Yang, K. Zhu, Y. Liu, G.G. Siu, Z.K. Xu, *Chin. Phys. Lett.* 25 (2008) 290–293.
- [22] F. Jiang, S. Kojima, *Jpn. J. Appl. Phys., Part 1* 38 (1999) 5128–5132.
- [23] A. Lebon, M. El Marssi, R. Farhi, H. dammak, G. Calvarin, *J. Appl. Phys.* 89 (2001) 3947–3954.
- [24] G. Xu, P.M. Gehring, G. Shirane, *Phys. Rev. B* 74 (2006) 104110–104116.